Magn Reson Mater Phy (2008) 21:87–94
DOI 10.1007/s10334-007-0092-0

RESEARCH ARTICLE

Optimized spectrally selective steady-state free precession sequences for cartilage imaging at ultra-high fields

O. Bieri · T. C. Mamisch · S. Trattnig · O. Kraff · M. E. Ladd · K. Scheffler

Received: 7 August 2007 / Revised: 27 September 2007 / Accepted: 26 October 2007 / Published online: 21 November 2007

Abstract
Object Fat suppressed 3D steady-state free precession (SSFP) sequences are of special interest in cartilage imaging due to their short repetition time in combination with high signal-to-noise ratio. At low-to-high fields (1.5–3.0 T), spectral spatial (spsp) radio frequency (RF) pulses perform superiorly over conventional saturation of the fat signal (FATSAT pulses). However, ultra-high fields (7.0 T and more) may offer alternative fat suppression techniques as a result of the increased chemical shift.
Materials and methods Application of a single, frequency selective, RF pulse is compared to spsp excitation for water (or fat) selective imaging at 7.0 T.
Results For SSFP, application of a single frequency selective RF pulse for selective water or fat excitation performs beneficially over the commonly applied spsp RF pulses. In addition to the overall improved fat suppression, the application of single RF pulses leads to decreased power depositions, still representing one of the major restrictions in the design and application of many pulse sequences at ultra-high fields.
Conclusion The ease of applicability and implementation of single frequency selective RF pulses at ultra-high-fields might be of great benefit for a vast number of applications where fat suppression is desirable or fat–water separation is needed for quantification purposes.

Keywords SSFP · Ultra-high fields · Water excitation · Fat suppression

Submitted to *MAGMA* for inclusion in the Special Issue on High Field MR as *New Concepts* paper.

O. Bieri (✉) · K. Scheffler
MR Physics, Department of Medical Radiology,
University of Basel, Petersgraben 4, 4031 Basel, Switzerland
e-mail: oliver.bieri@unibas.ch

T. C. Mamisch
Orthopedic Surgery Department, Inselspital, Bern, Switzerland

S. Trattnig
MR Center, Department of Radiology,
Medical University of Vienna, Vienna, Austria

O. Kraff · M. E. Ladd
Erwin L. Hahn Institute for Magnetic Resonance Imaging,
University Duisburg-Essen, Essen, Germany

Introduction

Motivated by the near linear increase in signal-to-noise ratios (SNR) with magnetic field strength (B_0), research and development of ultra-high-field whole body systems (7.0 T and above) is progressing rapidly. Particularly, musculoskeletal imaging benefits from improved image quality, contrast, and resolution at higher field strengths as compared to 1.5 T, as higher resolution may improve diagnostic accuracy and confidence [1–3]. Whereas state-of-the-art MRI is just becoming well-established at 3.0 T in academic and clinical settings, the availability of ultra-high-field whole-body MRI systems provides an excellent opportunity to explore high resolution morphologic and functional imaging of the musculoskeletal system [4].

In musculoskeletal systems, fat is often found adjacent to or interspersed within the tissues of interest, and it has been shown that especially at ultra-high-field systems the chemical shift artifact may significantly influence and degrade image quality [4]. Elimination of the chemical shift artifact, however, requires increased receiver bandwidths which in turn result in an overall reduced SNR. In addition, various clinical studies have demonstrated that fat suppression may enhance diagnostic information to detect musculoskeletal abnormalities with an accuracy equivalent to arthroscopy [5]. Moreover, fat suppression eliminates the need for high bandwidths to suppress chemical shift artifacts and thereby enables the detection of signal changes with increased SNR. This has led to an increased clinical usage of fat suppressed sequences for musculoskeletal imaging, preferably in 3D for high SNR [6]. Compared to 2D techniques, 3D sequences not only offer increased SNR but may also offer isotropic spatial resolution for multi-planar image reconstruction schemes, for improved morphologic assessment of small structures, or for reducing partial volume effects, e.g., for assessment of trabecular bone microarchitecture.

In general, selective excitation or suppression of water or fat bases on the frequency shift of the methylene protons in long chains of fatty acids of about 3.4 ppm below that of water protons. Several techniques have been presented to selectively excite or suppress water or fat with or without spatial selection [7]. Conventional fat suppression techniques are often based on spectrally selective radio-frequency (RF) pulses (so-called FATSAT pulses) to presaturate the signal from the lipids. Here, a narrow-band RF pulse selectively excites lipid protons, and the resulting transverse magnetization is then subsequently spoiled by gradient pulses before image acquisition [8]. A major disadvantage of this technique is the additional time required for the RF and gradient prepulses.

In addition, FATSAT pulses are incompatible with steady-state free precession (SSFP) sequences (except for the case of balanced SSFP [9]), such as the double-echo steady state (DESS) sequence and many others that have gained increased popularity in musculoskeletal imaging owing to short acquisition times in combination with high SNR [10,11]. Here, preparation pulses will interrupt the continuous flow of transverse and longitudinal steady states and thereby induce echo amplitude fluctuations that may lead to image artifacts and modified image contrast. This is not a severe problem in the T1-weighted, RF-spoiled SSFP-FID (FLASH) sequence, where a loss of coherent steady states may even improve the T1-weighted contrast. However, the more T2-weighted the SSFP, such as the SSFP-echo (PSIF) or the combined-echo SSFP (DESS), the more sensitive the sequences are to modifications.

Water (or fat) selective spectral-spatial (spsp) excitation pulses [12] can be implemented for clinical use into any kind of SSFP sequence in conjunction with slice-(2D) or volume-(3D)selective magnetic field gradients [7]. At low-to-high fields, spsp pulses are increasingly used because they offer shorter TRs and are less sensitive to magnetic field inhomogeneities than FATSAT preparations [7]. While susceptibility-related field inhomogeneities can be confined to 100–200 Hz even at 7 T the chemical fat–water shift amounts to ∼1,040 Hz as compared to ∼440 Hz at 3 T and ∼220 Hz at 1.5 T. As a result, especially at ultra-high fields, alternative selective water excitation schemes may become applicable that are too time-consuming at low fields. In this article, spsp efficiency for SSFP sequences at high field strengths is revisited. We will show that the high chemical shift at 7.0 T enables the application of a single, frequency selective RF pulse for either water or fat excitation. In contrast to the common spsp excitation scheme, the frequency selection resulting from single RF excitation is more effective and provides improved and more homogeneous fat suppression over the entire imaged volume. Moreover, the application of single RF pulses leads to decreased power depositions and thus to an overall reduced specific absorption rate (SAR), which still represents a major restriction for many pulse sequences at ultra-high fields.

Materials and methods

Measurements and calibrations were performed on a Magnetom 7 T whole body system (Siemens Medical Solution, Erlangen, Germany) equipped with actively shielded magnetic field gradient coils of 200 mT/m per ms slew rate with maximal amplitude of 45 mT/m in the longitudinal and 40 mT/m in the horizontal and vertical directions. All numerical simulations, data analysis and visualization were done using Matlab 7.0 (The MathWorks, Inc., Natick, MA, USA). The study was approved by the local ethics committee, and written consent was obtained prior to scanning.

Spectral selective RF pulse design

Spectral-spatial pulse design bases on a train of N subpulses (separated by ΔT) with tip angles (α_i). The N tip angles α_i can be calculated, e.g., using binomial coefficients [13]. Whereas first order binomial excitations (e.g., 1–1) are short, the sinusoidal spectral character of the excitation profile offers only limited fat suppression. Higher-order binomials (e.g., 1-3-3-1) offer better fat suppression but at the cost of significantly increased repetition and echo times. Often, a good compromise between better fat suppression and moderately increased TR is offered by second-order binomial (e.g., 1-2-1) RF pulses, as displayed in Fig. 1a.

The excitation spectrum is periodic with a period of $1/(\Delta T)$ Hz, i.e., with the inverse of the RF subpulse spacing (see Fig. 1a). Thus, selective excitation of water protons without touching the fat is granted for

$$1/\Delta T = (2 \cdot \Delta v)/(2n - 1), \quad n \in N \tag{1}$$

where Δv is the water-fat frequency shift. Spectral-spatial pulses can be applied with either positive (unipolar) or positive and negative (bipolar) gradient lobes (as displayed in Fig. 1a). Alternating gradient lobes clearly offer minimal interpulse spacing (no slice refocusing is needed) and thereby

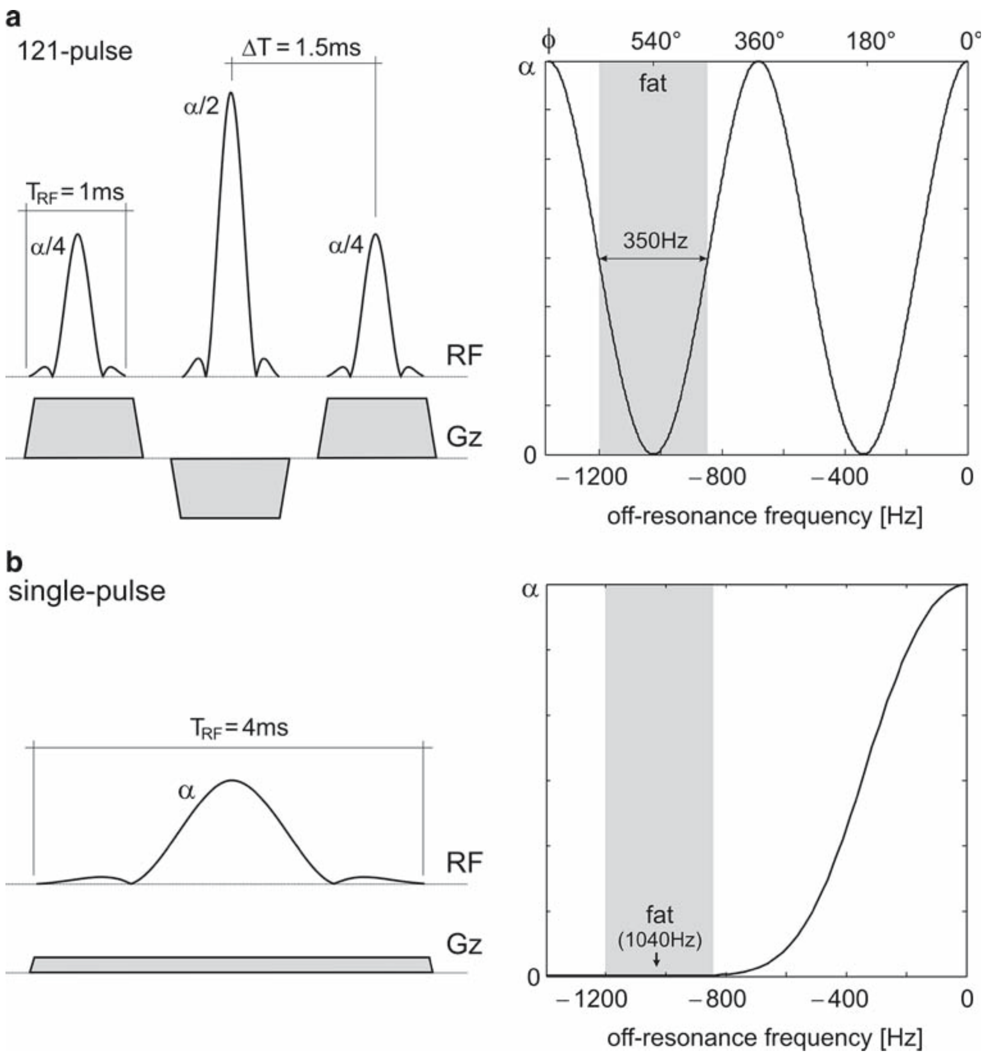

Fig. 1 Spectral-spatial excitation schemes. **a** Binomial excitation pulses (e.g., 1–2–1) for selective excitation as commonly applied at low-to-high field strengths. Typically, spsp subpulses have duration $T_{RF} \sim 1$ ms or even more. At 7.0 T, fat is shifted by about −1,040 Hz from the water resonance, i.e., roughly one cycle/ms. Thus, the conventionally applied 180° phase advance ($\Delta T = 0.5$ ms) has to be increased to 540° ($\Delta T = 1.5$ ms) due to subpulse limitations ($T_{RF} < \Delta T$, see Eq. 2). **b** Frequency selectivity by a single RF excitation. For small tip angles ($\alpha \ll \pi$), excitation (**b**, *right*) is proportional to the frequency spectrum, and selectivity is thus proportional to the overall pulse duration (see Eq. 3). Note that both spsp excitation schemes have essentially identical durations (at 7 T)

minimal preparation times; however, selective excitation is more prone to system imperfections, such as flow or gradient distortions, as compared to unipolar excitations.

From Eq. (1) and Fig. 1 it is evident that the subpulse duration T_{RF} is limited to

$$T_{RF} < \Delta T = (n - 0.5)/\Delta v \qquad (2)$$

From this, at 7.0 T, the minimum ($n = 1$) subpulse duration should be less than 500 µs for water or fat selective excitation, which seems impracticable from usual SAR limitations. As a result, the phase advance must be increased from 180° (i.e., one half turn with $\Delta T = 0.5$ ms) to 540° (i.e., one and a half turns with $\Delta T = 1.5$ ms), as displayed in Fig. 1a. The subpulse duration was fixed to $T_{RF} = 1.0$ ms to account for finite rise-time limitations of the slice selection gradients.

In Fig. 1b, the frequency bandwidth of a single RF pulse of moderate duration ($T_{RF} = 4.0$ ms) is shown. Essentially the same RF pulse envelope (Hamming-filtered sinc-pulse with one side maximum) as for the binomial subpulses was used (Fig. 1a). In contrast to the spsp pulses, the spectrum of a single RF pulse is not periodic but confined to a single transition region. From this, excellent selectivity can be expected within the volume of interest. For low flip angles, the frequency response profile is nearly identical to the excitation profile. Thus, the pass-band transition width, $\Delta\nu_{RF}$, is closely related to the duration of the RF pulse itself, i.e.,

$$\Delta\nu_{RF} \sim 1/T_{RF} \qquad (3)$$

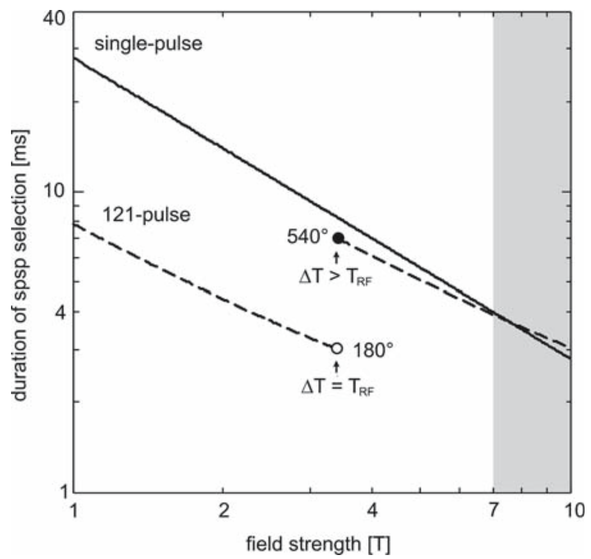

Fig. 2 Duration of the spsp excitation schemes as presented in Fig. 1 as a function of main magnetic field strength. At low-to-high field strengths (1.0 to about 3.4 T), the time needed for selective excitation differs by almost a factor of 5. Spectral-spatial excitation from a single RF pulse seems impracticable due to exceedingly long excitations ($T_{RF} \sim 20$ ms at 1.5 T, see *solid* line) that may hamper proper slice selection from relaxation effects or other system imperfections such as field inhomogeneities. With increasing field strength, however, the time needed for the 180° phase advance for binomial excitation (*dashed* line) falls below the subpulse spacing (at 3.4 T for the preparation displayed in Fig. 1a), forcing an increase in the phase advance to 540°. In combination with the decreasing preparation time for single RF frequency selectivity with field strength (see Eq. 3), similar preparation times are achieved at ultra-high fields (>7.0 T)

At 1.5 T, the chemical shift between water and fat is about 220 Hz, yielding a single pulse RF duration for spectral selectivity on the order of ∼20 ms (for a time-bandwidth product of about 2) and thus impractical at low fields. However, this changes completely at ultra-high fields since the RF time is inversely proportional to the bandwidth and thus to the field strength (Eq. 3). Here, the time needed for water selection from single pulses drops even below the spsp preparation time (Fig. 2). Whereas at low to high fields, spsp preparation is by far more time efficient (∼5 times), the demand of a bigger phase advance from subpulse duration constraints cancels this advantage at high to ultra-high fields (see Eq. 2), and spsp preparation becomes more time consuming at field strengths of 7.0 T and above.

Potential spsp optimization strategies, such as phase modulation [6], would decrease the delay between the subsequent RF subpulses and thereby improve the time efficiency, but only at the cost of a somewhat reduced tip angle (α). This might not be so problematic at low fields; however, at ultra-high fields, SAR issues are one of the major restrictions for the design of sequences, since

$$\mathrm{SAR} \propto B_0^2 \cdot \alpha^2 \cdot \Delta\upsilon_{\mathrm{RF}} \tag{4}$$

for non-adiabatic pulses [14]. We, therefore, prefer to use a 180°, i.e., a 540°, phase advance at 7.0 T, so as to not lose too much RF power efficiency, and deliberately compare the two spsp methods on a more qualitative basis. Compared to the single RF pulse excitation, SAR is increased by 50% with second-order binomial application. The overall achievable SAR reduction depends also sensitively on the order of the binomials used and increases further with increasing order.

It might be noteworthy (and being evident from Fig. 1b) that single, e.g., water-selective, RF pulses also excite fat in a nearby volume (i.e., where the slice selection gradient shifts the local frequency by +1,040 Hz). Thus some care should be taken when designing single RF spsp selectivity to avoid an overlay of nearby fatty structures on actual water-only images. For 3D volumes, however, this does not represent a critical issue since such unintended excitations can be easily shifted either outside of the imaged object (as for the human knee) or outside of the sensitivity area of local transmit/receive coil. Spatial selectivity from single RF pulses can, thus, be rather seen as a result of a smart arrangement of the FOV or of the spatial sensitivity of the coils used.

From Fig. 1, slab selection gradients for single RF excitations are reduced as compared to binomial excitation schemes (∼0.1 mT/m for 150 mm slab thickness) and the slab profile might thus show some increased sensitivity to local susceptibility gradients; especially for large volumes. Spectral spatial slab selection, however, is modulated by the frequency response function as displayed in Fig. 1a, and as a result, the constraint on the field homogeneity within the 3D slab is even less for the single RF pulse excitation (∼800 Hz) as compared to spsp selection (∼350 Hz).

Imaging protocols

Volume shimming and frequency adjustments were applied prior to data acquisition. A CP transmit/receive (TX/RX) extremity coil (Invivo, Gainesville, FL, USA) was used for sagittal knee joint images, whereas a 10-cm-diameter single loop TX/RX surface coil (Rapid Biomedical, Würzburg, Germany) was used for the generation of axial images of the distal femur. If possible, receiver bandwidths greater than 250 Hz/pixel were applied in non-selective imaging protocols for reduction of chemical shift artifacts [4]. Special spectral pulses as displayed in Fig. 1 were implemented in SSFP-FID (FISP, FFE, GRASS), SSFP-echo (PSIF, CE-FAST, T2-FFE) and in the DESS sequence to allow image acquisitions with or without spsp selectivity. Only 3D image acquisitions were considered and the same preparation time was used for both excitations, enabling the use of essentially identical imaging protocols. For the axial 3D imaging protocols, the local sensitivity from the surface coil (limited FOV) was used to suppress any outer-slab fat or water excitation, whereas for the sagittal acquisitions, the spatial extend of the slab selec-

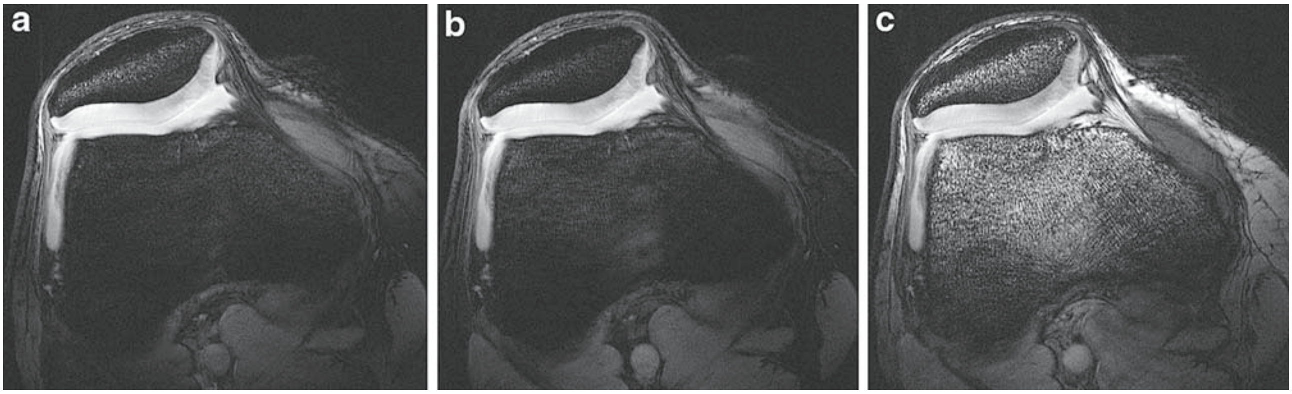

Fig. 3 Axial 3D DESS images of the patella of the knee joint at 7.0 T using a surface single loop coil. **a** Water selection from binomial excitation as presented in Fig. 1a, and **b** based on single RF pulse excitation as presented in Fig. 1b. As a reference, unselective excitation is shown in Fig. 1c. From visual inspection, both spsp excitation schemes provide almost identical high quality fat-free images. Images (44 slices) were acquired within 7.5 min with 200 μm × 200 μm × 3,000 μm resolution [$\alpha = 30°$, 265 Hz/pixel receiver bandwidth, TE/TR = 6.7/17.2 (ms)]

tion covered the whole knee. The reader is referred to the individual figure captions for the corresponding acquisition parameters used.

Results and discussion

First, the performance of water selective excitation is compared based on human knee DESS images in vivo. Figure 3a, b display sample fat-free images from either spsp binomial excitation as presented in Fig. 1a or from single RF pulses as displayed in Fig. 1b. Bright signal intensity can be observed from the patella, whereas signal from subcutaneous fat and fat in trabecular bone is highly and homogenously suppressed except for minor residual fat signal in Fig. 3a. For reference, an image with unselective excitation is shown in Fig. 3c. A direct comparison of the two selective excitations reveals no apparent differences in the depiction of the patella and only sparse differences in the surrounding tissue (differences are mainly found in the incomplete suppression of fatty tissues and in the representation of the cruciate ligament). In both images cartilage surface defects, an early sign of osteoarthritic changes to the cartilage, are clearly depicted and indicate the potential of high field imaging for improved cartilage diagnosis using fat-saturation. These images substantiate the high similarity between the two frequency selective methods at 7.0 T, especially for small areas of interest or for reduced FOV sensitivities from small surface coils, where the limited volume of interest allows for low variations in the main magnetic field. Reduced field inhomogeneities are beneficial for unwanted excitations from side lobes in spsp pulses that may impair the quality of fat suppression.

From Fig. 1, owing to the 540° phase advance constraint at high fields, the spsp transition bandwidth is decreased by a factor of three as compared to 180° at low magnetic field strengths. In addition, second-order binomials still result in near sinusoidal excitation profiles with full amplitude half-width of about 170 Hz, i.e., yielding about 10% signal variation within ±70 Hz from the wedge-shaped minima or maxima. In contrast, frequency selectivity from a single RF pulse clearly performs superiorly to spsp excitations, not only from the provided full chemical shift for frequency selectivity, enabling broader spectral selection, but also from a more uniform and pronounced widespread suppression. Clearly, this should result in more homogeneous spectral selections from single RF pulses, especially for targets or larger FOVs that exhibit increased field inhomogeneities or susceptibilities.

Deficiencies from unwanted spectral selections for spsp pulses from large and inhomogeneous volumes become apparent in sagittal images of the human knee joint, as displayed in Fig. 4. Here, the available broad frequency selectivity of single RF pulses in combination with the non-oscillating excitation spectrum provides an excellent selective excitation (slab selection profile) or fat suppression even for increased field inhomogeneities as generally observed at ultra-high field strengths. The narrowed spectral water selective bandwidth for spsp binomial pulses (see Fig. 1) may even result in an incomplete depiction of the anterior cartilage (Fig. 4). From this it can be concluded that selective excitation from the use of a single but somewhat prolonged RF pulse performs superiorly to spsp excitation schemes and provides high quality fat-free images at 7.0 T. This superiority might be even more pronounced for abdominal imaging or other targets where even larger and more severe field inhomogeneity issues might be present.

In principle, spsp pulses can be employed to either selectively excite water or selectively excite fat. Especially assessment of trabecular bone microarchitecture, an important indicator for bone fracture risk, bases on a quantitative a

b

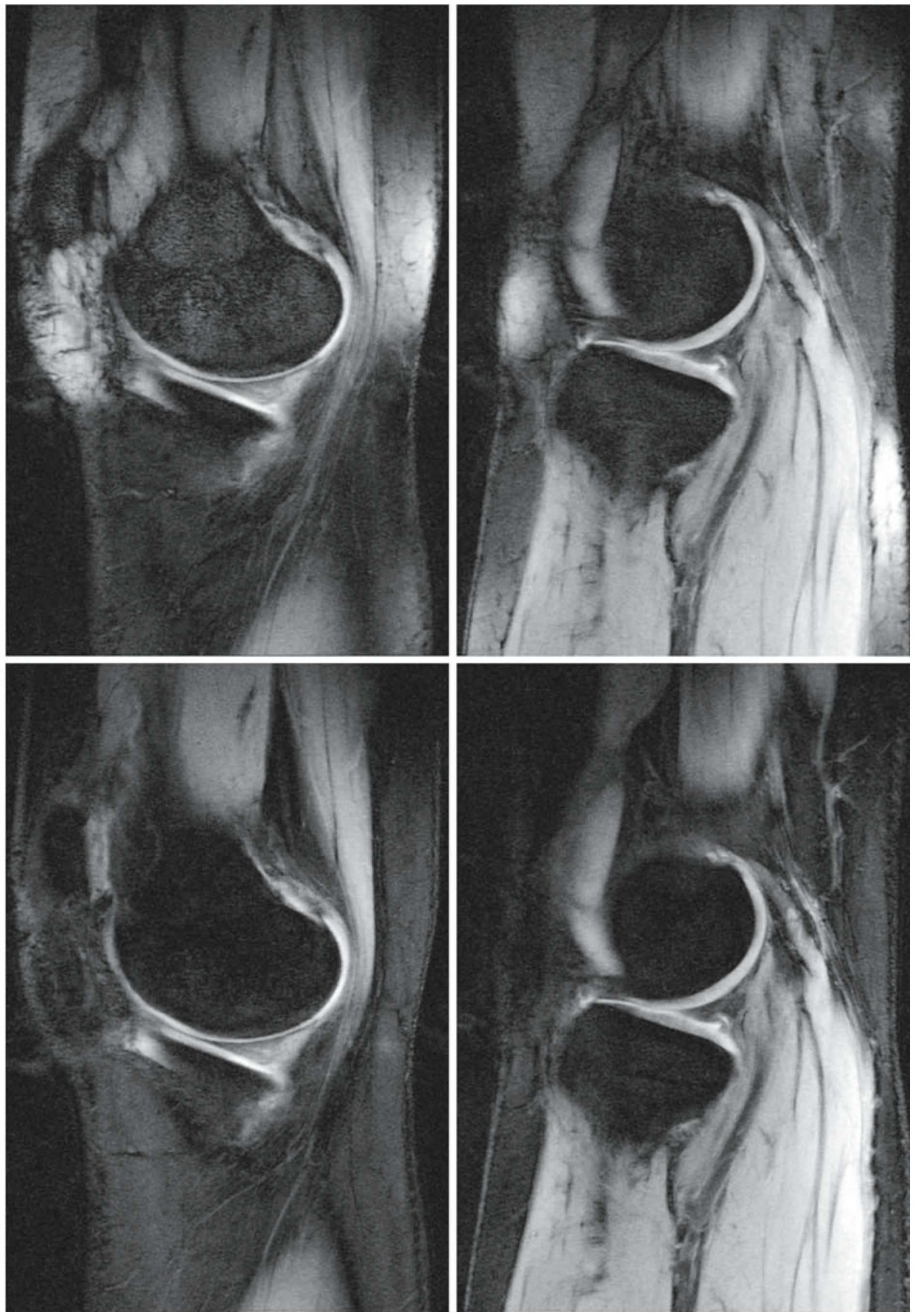

Fig. 4 Sagittal water-selective 3D DESS imaging of the human knee joint at 7.0 T using a CP volume coil and binomial (**a**) or single RF pulse excitation (**b**). In contrast to Fig. 3, the larger FOV sensitivity of the CP coil reveals incomplete fat suppression for spsp binomial preparation (trabecular bone marrow, fatty tissue) as a result of its limited transition bandwidth (∼350 Hz, see Fig. 1a). Single pulse excitation, however, clearly benefits from its widespread suppression (see Fig. 1b) to deliver robust high quality fat-free images. Likewise, the extended excitation bandwidth can improve overall depiction of cartilage. Images (72 slices) were acquired within ∼8 min with 300 μm × 300 μm × 3,000 μm resolution [$\alpha = 30°$, 360 Hz/pixel, TE/TR = 5.7/14.3 (ms)]

analysis of fatty bone marrow. Whereas bone marrow appears bright on a fat-only image, fat-free trabecular bone images have vanishing amplitudes as a result of the very short T2 times (∼250–500 μs). Shifting the main RF pulse frequency 1,040 Hz away from the water resonance makes spsp pulses (Fig. 1) selective to fat. Thus, two images may be acquired: one displaying water and the other displaying fatty tissue only (Fig. 5). As might be expected from the overall excellent water-only excitation performance of single RF pulses (see Figs. 3, 4), separation into water- and fat-only components (Fig. 5b) can be easily accomplished with high robustness and quality.

The DESS protocol provides images with T2 contrast from the superposition of two echo acquisitions within each TR, namely the readout of the SSFP-FID and the SSFP-echo signal. The latter is responsible for the T2-weighting, whereas the SSFP-FID amplitude delivers a T1-contrast, similar to the frequently used RF spoiled fast low-angle shot (FLASH) sequence for musculoskeletal imaging. Spectral-spatial imaging as presented in Fig. 1 can be easily imple-

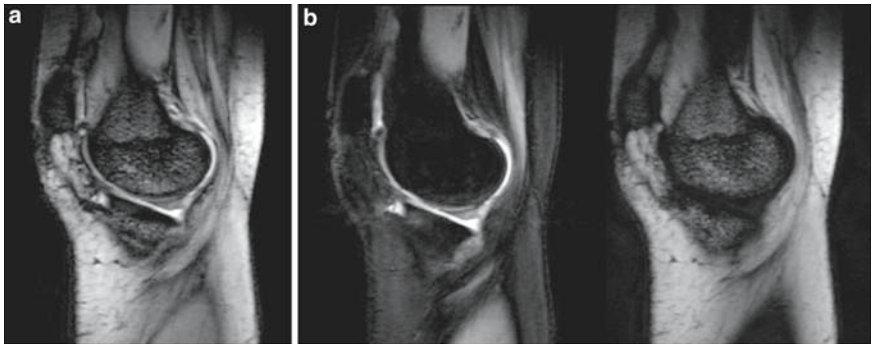

Fig. 5 Sagittal sample images of a 3D DESS acquisition of the human knee at 7.0 T using a CP coil. **a** Non-selective excitation showing both, i.e., water and fat, components. **b** Water and fat separation based on single RF excitation. **b** *Left* centering excitation at the water resonance yields a water-only image, whereas *right* a fat-only image is acquired from a simple shift of the central excitation frequency to the fat resonance, i.e., −1,040 Hz relative to the water resonance. Component images (36 slices) were acquired within 1.5 min ($\alpha = 30°$, 360 Hz/pixel receiver bandwidth, TE/TR = 5.7/14.3 (ms), 800 μm × 800 μm × 3,000 μm resolution)

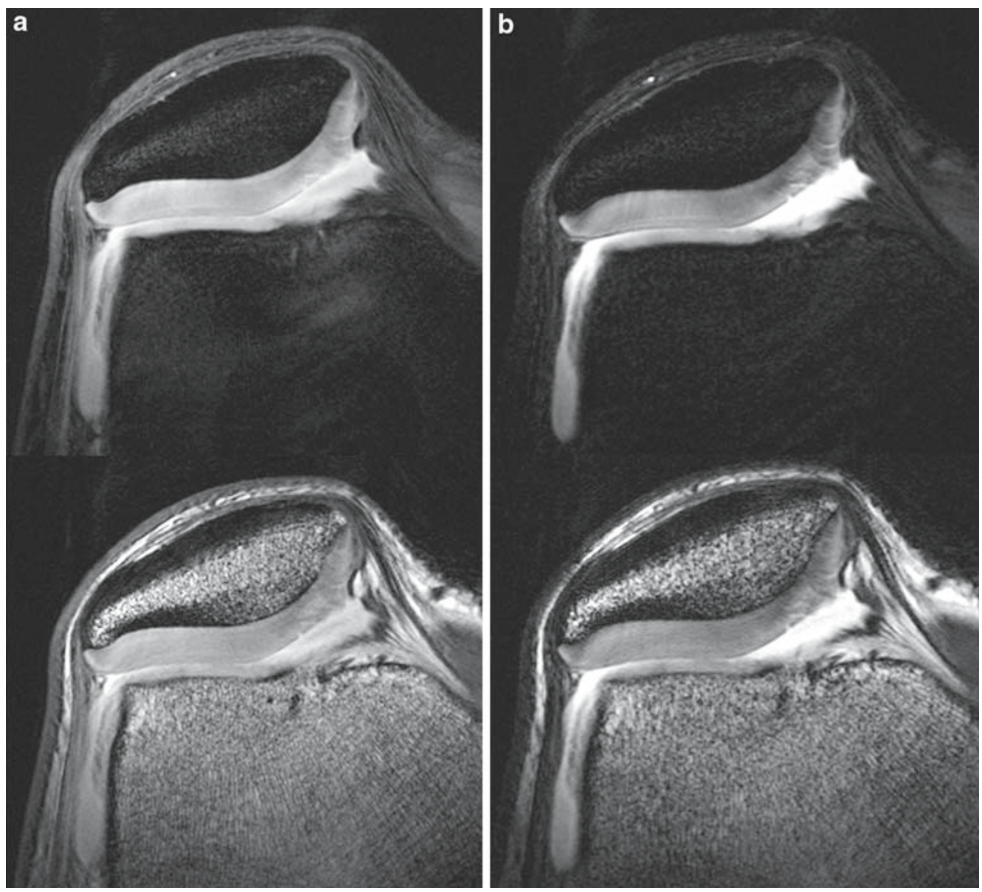

Fig. 6 Axial 3D SSFP-FID **a** and SSFP-echo **b** images (280 μm × 280 μm × 3,000 μm) of the patella of the knee joint at 7.0 T using a surface single loop coil. Water-fat unselective images (40 slices) were acquired within 3.5 min ($\alpha = 30°$, 320 Hz/pixel, TE/TR = 3.0/6.9 (ms), using $T_{RF} = 600\ \mu s$), whereas fat-free images were acquired within 5 min ($\alpha = 30°$, 320 Hz/pixel, TE/TR = 4.7/10.3 (ms), using $T_{RF} = 4,000\ \mu s$). Early fissures through the cartilage layer are visualized on the scan achieved at 7 T

mented with any kind of SSFP sequence. In Fig. 6, the results from simple RF pulse prolongation as given in Fig. 1b are displayed for both SSFP-FID (Fig. 6a) and SSFP-echo (Fig. 6b). The increased fluid-cartilage contrast in the patella for the SSFP-echo compared to the SSFP-FID is clearly visible. In accordance with our previous results from the DESS sequence (see Fig. 3), spsp single pulse excitation yields high quality fat-free images. However, unselective excitation of both water and fat protons is revealed for short RF durations (0.5–1 ms) where the spectral bandwidth of the single pulse is similar to the overall chemical shift.

In summary, at ultra-high magnetic field strengths, SSFP sequences can be made either water or fat selective by simple RF pulse prolongation. RF pulse prolongation decreases the overall pulse excitation frequency bandwidth proportional to the prolongation itself. As a result, at low-to-high fields, the time needed for selective excitation from a single RF pulse is far greater than that required for commonly applied spsp binomial pulses and repetition times are considerably increased. At ultra-high fields, however, the RF duration needed for spectral selectivity is on the order of or even below the time required for spsp excitation based on binomials. Besides the overall better performance for delivering high quality fat-free images with high robustness, application of single RF pulses for spsp frequency selection offers reduced SAR. Consequently, this type of selective water excitation may offer great benefit and be of interest for all ultra-high-field applications that are based on SSFP-type sequences.

Conclusion

We have given evidence that the spsp pulses commonly used with SSFP-type sequences at low-to-high fields are surpassed by the application of single RF frequency selective pulses at ultra-high-field MRI systems. Single frequency selective RF pulses are as time efficient as spsp-related preparations but yield excellent and robust suppression or excitation, deliver low RF power, and are thus highly applicable at ultra-high-field systems. Although we have only demonstrated implementation for SSFP, it is noteworthy that our results can be readily transferred to other fat suppression techniques such as the common FATSAT preparation schemes in RF-spoiled FLASH or other preparation blocks. In particular, the ease of applicability and implementation might be of great benefit for a vast number of other applications where fat suppression is desirable or fat–water separation is needed for quantification purposes.

References

1. Kuo R, Panchal M, Tanenbaum L, Crues JV 3rd (2007) 3.0 Tesla imaging of the musculoskeletal system. J Magn Reson Imaging 25(2):245–261
2. Saupe N, Pfirrmann CW, Schmid MR, Schertler T, Manestar M, Weishaupt D (2007) MR imaging of cartilage in cadaveric wrists: comparison between imaging at 1.5 and 3.0 T and gross pathologic inspection. Radiology 243(1):180–187
3. Masi JN, Sell CA, Phan C, Han E, Newitt D, Steinbach L, Majumdar S, Link TM (2005) Cartilage MR imaging at 3.0 versus that at 1.5 T: preliminary results in a porcine model. Radiology 236(1):140–150
4. Regatte RR, Schweitzer ME (2007) Ultra-high-field MRI of the musculoskeletal system at 7.0 T. J Magn Reson Imaging 25(2):262–269
5. Hardy PA, Recht MP, Piraino DW (1998) Fat suppressed MRI of articular cartilage with a spatial-spectral excitation pulse. J Magn Reson Imaging 8(6):1279–1287
6. Thomasson D, Purdy D, Finn JP (1996) Phase-modulated binomial RF pulses for fast spectrally-selective musculoskeletal imaging. Magn Reson Med 35(4):563–568
7. Zur Y (2000) Design of improved spectral-spatial pulses for routine clinical use. Magn Reson Med 43(3):410–420
8. Rosen BR, Wedeen VJ, Brady TJ (1984) Selective saturation NMR imaging. J Comput Assist Tomogr 8(5):813–818
9. Scheffler K, Heid O, Hennig J (2001) Magnetization preparation during the steady state: fat-saturated 3D TrueFISP. Magn Reson Med 45(6):1075–1080
10. Hardy PA, Recht MP, Piraino D, Thomasson D (1996) Optimization of a dual echo in the steady state (DESS) free-precession sequence for imaging cartilage. J Magn Reson Imaging 6(2):329–335
11. Eckstein F, Hudelmaier M, Wirth W, Kiefer B, Jackson R, Yu J, Eaton CB, Schneider E (2006) Double echo steady state magnetic resonance imaging of knee articular cartilage at 3 Tesla: a pilot study for the osteoarthritis initiative. Ann Rheum Dis 65(4):433–441
12. Meyer CH, Pauly JM, Macovski A, Nishimura DG (1990) Simultaneous spatial and spectral selective excitation. Magn Reson Med 15(2):287–304
13. Hore P (1983) Solvent suppression in Fourier transform nuclear magnetic resonance. J Magn Reson 55:283–300
14. Bernstein M, King K, Zhou X (2004) Handbook of MRI pulse sequences. Elsevier, Amsterdam